Implementation of a Permanent Magnet Synchronous Motor Drive System in a Suspended Trolley Machine

E. Falcon, S. Sørensen, S. Pellegrino

Department of Materials and Production, Aalborg University
Fibigerstraede 16, DK-9220 Aalborg East, Denmark
Email: efalco17@student.aau.dk,
Web page: http://www.mechman.m-tech.aau.dk/

Abstract
This paper investigates the implementation of a permanent magnet synchronous DC motor in an automated cow feeding machine that runs on a monorail hung from barn roofs. The project approaches the problem as the design of a stand-alone module to be implemented in similar machines. The goals of the project are improved efficiency, improved performance and reduced maintenance. This is done through re-design of the power transmission system, the motor technology, and the control of the system. In addition, care is taken in terms of the braking capabilities of the system in relation to slopes, and the characteristics of the available batteries evaluated.
The feeding machine which the drive module is being designed for is a multiple ton trolley with a Lead-Acid battery pack, a holding area for the feed, a bale shredder, and conveyor belts for food distribution. The trolley is suspended from the drive modules on the front and back through flexible linkages.
The transmission system is changed from a worm-gear to a more direct and lower ratio gearing. As the worm-gear provides a braking functionality, a friction brake is added to provide braking force when power is removed from the motor.
The main component of the project is the implementation and control of a permanent magnet synchronous motor which includes the selection and modeling of the motor and the use of a frequency converter to drive the motor with the desired performance while maintaining efficient operation.

Keywords: Permanent Magnet Synchronous Motor(PMSM); Cascade Control; Monorail Trolley;

1. Introduction

GEA Mullerup is a subset of GEA Group that makes farm equipment specifically tailored for use with cows. The product of interest for this project is a suspended feeding trolley for the automated distribution of food to the cows on a farm. The machine consists of bale shredders, conveyor belts for food distribution, and the drive modules that move the trolley. The trolley have two drive modules with which the machine is suspended from the rail. In the working environment, the rails the machine is suspended from are allowed to have a maximum grade of 2%, it is however not uncommon to see a slope of up to 5% grade in potential applications. The machines range in weight from 1000 $[kg]$ unloaded to 2200 $[kg]$ loaded with the heaviest type of feed. The typical usage period of the trolley is 12 hours per day. The component of interest in this project is the drive system on rails that moves the machine which will henceforth be referred to as a "Drive Module"

The transmission of the drive modules consists of a Direct Current (DC) motor, a $25:1$ worm gearbox and a belt drive, which create the forward motion of the machine.

2. Concept Development

To determine improvements of the current drive module a concept design was conducted. A parameter of the concept design was to implement a permanent magnet synchronous motor (PMSM) into the drive module. Through the concept design is was determined to implement a MagicPie Edge hub motor as it had a combination of the torque and velocity required to replace both the DC motor and the worm gear. A belt drive is deemed necessary to transfer the power from the hub motor to the wheels on the rails.

3. Modeling of the Existing System

For the purpose of comparing the motion of the drive module with the implemented PMSM to the drive module in the existing system, a model must be created.

3.1 DC Motor Model

The equations used to model the DC Motor are[1]:

$$V = E_a + i_a \cdot R_a \tag{1}$$
$$E_a = k_a\phi \cdot \omega_m \tag{2}$$
$$\tau_m = k_a\phi \cdot i_a \tag{3}$$

The model of the DC motor is used in order to identify the energy losses in the existing transmission system.

3.2 Pendulum Motion

The trolley is suspended from the rail by chains and pivoting joints that enable it to swing. An oscillating pendulum with a mass of up to two tons, can be a harm to humans around the wagon, puts extra stress on mechanical parts, and affects the loading of the motor. The two arms connecting the drive module to the wagon are enforced to be parallel by a strut. To be able to control this pendulum, a model describing the angle of the wagon to the vertical line θ_p, dependant on the acceleration of the drive module is used. The whole pendulum with the system can be seen in figure 1.

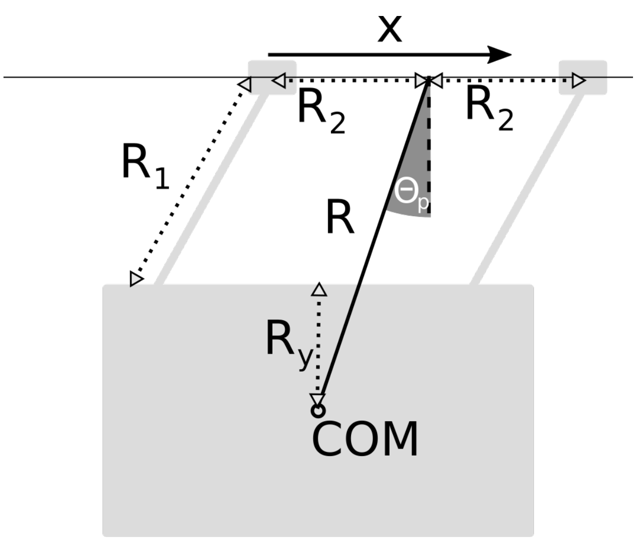

Fig. 1 Schematics of the Pendulum

4. Tests on existing System

The current drive module is made up of several components, where each component causes losses in the transmission of power through the system. These losses are quantified in order to determine the efficiency of the system. The experiments to determine the losses of the system include no load testing of the motor, no load and loaded testing of the gearbox, and no load testing of the belt drive.

4.1 No Load Test

The no load test is used to determine losses in the drive module. The test is conducted through application of various voltage levels up to the maximum of $24[V]$ with the angular velocity and current at each iteration recorded. The angular velocity and the current are first recorded once it is certain the motor is at steady state. From the voltage, current, and angular velocity, the motor constant $k_a\phi$ and the losses can be identified. The torque friction of the motor is calculated as:

$$\tau_{motor} = \frac{V \cdot i_a - R \cdot i_a^2}{\omega_m} \tag{4}$$

And the motor constant $k_a\phi$ as:

$$k_a\phi = \frac{V + i_a \cdot R_a}{\omega_m} = 0.104\left[\frac{V}{rad/s}\right] \tag{5}$$

When subtracting the results from the no load test with the gearbox from the no load test with only the motor, torque friction of the gearbox can be estimated as depicted in figure 2. The same is then done for determine the friction losses in the belt drive.

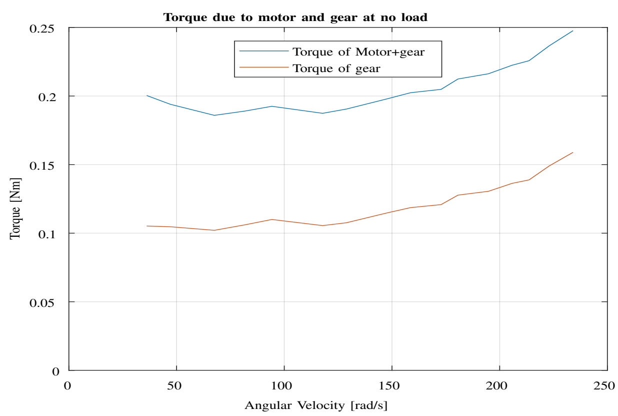

Fig. 2 Torque due to motor and gear at no load

4.2 Loaded Test

By placing a mass hanging from the worm gearbox, a load was added. By measuring the velocity v of the mass m the output power was calculated.

$$P_{output} = v \cdot m \cdot g \tag{6}$$

When combining the results of the loaded and no-load test, it is possible to obtain the torque caused by losses during loading the system as in figure 3.

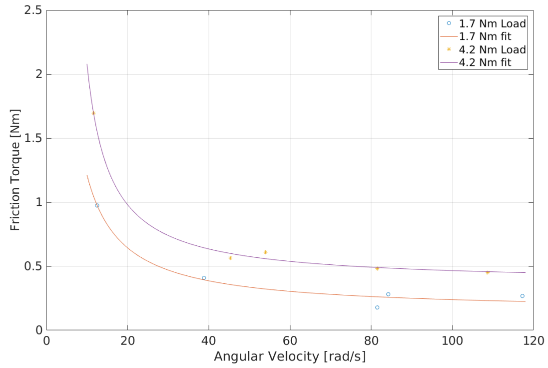

Fig. 3 The friction torque in the DC Motor due to loading

5. Mechanical Design

The design for the mounting of the hub motor was inspired from the tensioning system currently in place on the existing system. The implementation of the PMSM is seen in figure 4.

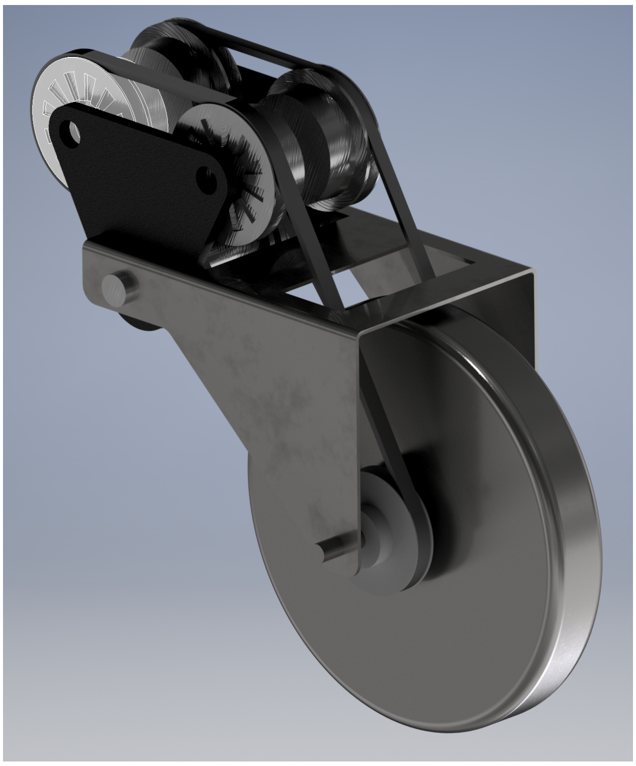

Fig. 4 Concept design for the mounting of the hub motor.

A simple finite element analysis was conducted to identify the maximum stresses in the structure. The stresses were found to be a maximum of

6. Permanent Magnet Synchronous Motor Modeling

The PMSM has permanent magnets on the rotor and windings on the stator. The permanent magnets generate a rotor magnetic field that creates a sinusoidal rate of change of the flux. The PMSM implemented has three coils, where each coil can be modelled by the classical voltage equation. The modeling is based on [2].

$$v = R \cdot i + L\frac{d}{dt}i + e \tag{7}$$

For all three coils it gives:

$$\begin{bmatrix} v_a \\ v_b \\ v_c \end{bmatrix} = \begin{bmatrix} R & 0 & 0 \\ 0 & R & 0 \\ 0 & 0 & R \end{bmatrix} \begin{bmatrix} i_a \\ i_b \\ i_c \end{bmatrix} + \begin{bmatrix} L_a & L_{ba} & L_{ca} \\ L_{ba} & L_b & L_{cb} \\ L_{ca} & L_{cb} & L_c \end{bmatrix} \frac{d}{dt} \begin{bmatrix} i_a \\ i_b \\ i_c \end{bmatrix} + \begin{bmatrix} e_a \\ e_b \\ e_c \end{bmatrix} \tag{8}$$

If all phases are symmetric, meaning the inductance and the mutual inductances are equal with a star connection the voltage equation can be simplified.

$$\begin{bmatrix} v_a \\ v_b \\ v_c \end{bmatrix} = \begin{bmatrix} R & 0 & 0 \\ 0 & R & 0 \\ 0 & 0 & R \end{bmatrix} \begin{bmatrix} i_a \\ i_b \\ i_c \end{bmatrix} + \begin{bmatrix} L-M & 0 & 0 \\ 0 & L-M & 0 \\ 0 & 0 & L-M \end{bmatrix} \frac{d}{dt} \begin{bmatrix} i_a \\ i_b \\ i_c \end{bmatrix} + \begin{bmatrix} e_a \\ e_b \\ e_c \end{bmatrix} \tag{9}$$

The model setup is currently in what's called the natural coordinates for the PMSM. The torque of a PMSM is directly proportional with the current in the quadrature axis on the rotor. To get from the natural coordinates of the stator, ABC, to the rotor reference frame, dq, a Clarke transformation as well as a Park transformation is conducted. The fixed stator reference frame, α, β can be chosen arbitrarily on the stator and is therefore chosen so the axis α aligns with coil a. The Clarke transformation is shown in Equation 10:

$$\begin{aligned} i_\alpha &= i_a \\ i_\beta &= \frac{2 \cdot i_b + i_a}{\sqrt(3)} \end{aligned} \tag{10}$$

Once the current of the fixed stator coordinate is known the Park transformation is used to get the current of the rotor reference frame. The Park transformation is shown in Equation 11

$$\begin{aligned} i_d &= cos\theta_e \cdot i_\alpha + sin\theta_e \cdot i_\beta \\ i_q &= -sin\theta_e \cdot i_\alpha + cos\theta_e \cdot i_\beta \end{aligned} \tag{11}$$

Where $theta_e$ is the electrical angle which can be derived from a measured angle, θ_m and the number of pole pairs, P, as described in equation 12

$$\theta_e = P \cdot \theta_m \tag{12}$$

From the current the voltage equations in the dq coordinate system are then calculated as:

$$V_d = R \cdot i_d + L_d \frac{di_d}{dt} - \omega_m L_q i_q$$
$$V_q = R \cdot i_q + L_q \frac{di_q}{dt} + \omega_m \cdot L_d \cdot i_d + \lambda_{pm} \cdot \omega_m \quad (13)$$

Where the couplings, $\omega_m \cdot L_d \cdot i_d$ and $\omega_m L_q i_q$ are assumed as disturbances. As the inductances, $L_d = L_q$, the torque is calculated as shown in Equation 14

$$T_e = \frac{3}{2} \cdot P \cdot \lambda_{pm} \cdot i_q \quad (14)$$

7. Control Design

In order for the machine to operate efficiently and effectively, controllers were designed in order to control the speed through the aforementioned direct and quadrature axis currents.

7.1 Requirements

As GEA does not have strict requirements for performance of the drive module, the goal of the control design was based on the performance of the current system as well as targeting improved efficiency.

The control targets are:

- Acceleration of the drive module to a speed of 20 $[m/min]$ within one meter.
- Peak current less than 20 $[A]$.
- Effective rejection of slope disturbances up to $\pm 2\%$ grade.

7.2 Controller Design

The control of the system is conducted through the use of cascade control as described in [3]. It is expected that the current responds at least 10 times quicker than the velocity. The control of the PMSM is seen in Figure 5 utilizing two PI controllers to control the currents in the d and q axes separately. In addition, the speed is controlled by a PI controller which provides the reference value to the q-current controller.

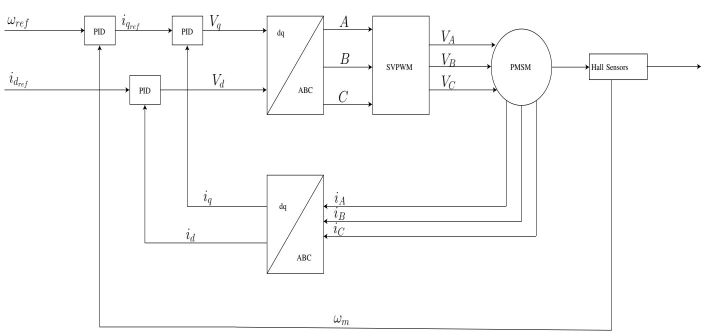

Fig. 5 Control of the PMSM.

7.2.1 *Current Controllers*

As the direct and quadrature axis inductances of the stator are assumed equal due to the surface mounted magnets in the MagicPie motor [4], the controllers for currents can be equal though their references are different.

The I_d controller has the purpose of reducing the direct axis current to zero as it only creates losses in the system.

The gains chosen for the i_d controller are $K_p = 120$ and $K_i = 1000$.

The I_q controller will be identical to the I_d controller and thus will also have controller values of $K_p = 120$ and $K_i = 1000$. With these controllers, the step response of the current settles within 0.4 $[ms]$ and has no overshoot.

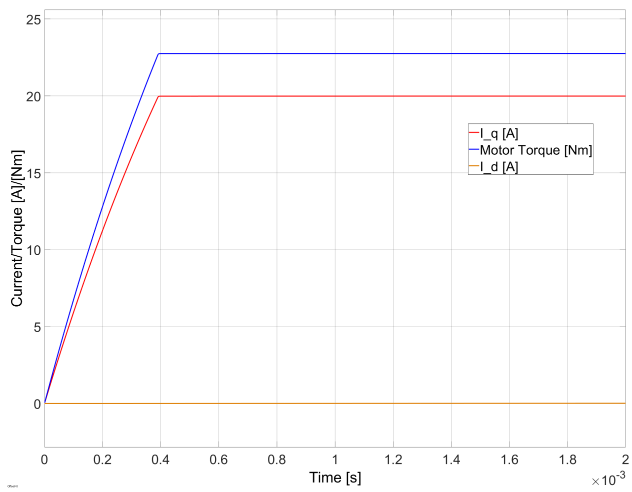

Fig. 6 Step response of current controllers with $I_{q_{ref}} = 20[A]$.

7.2.2 *Speed Controller*

The speed controller was developed based on the targets of high efficiency and acceleration to maximum speed within one meter. As the efficiency of the motor is inversely proportional to the current, due to the resistive losses, a lower rate of acceleration is advantageous.

The controller gains were adjusted by hand and prioritized the reduction of total energy over the curve instead of the time to the operating speed. The speed reference used is the current peak travel speed used for traveling longer distances of 20 $[m/min]$ or 0.33 $[m/s]$. As this speed is the travel speed, the overshoot does not matter and is thus ignored other than the energy contribution.

7.3 Trajectory Planning

In order to test the speed controllers and to improve the efficiency of operation, various acceleration trajectories were tested on a nonlinear model. For each trajectory tested, controllers were developed that would allow for the machine to reach the operating velocity at the same time as the acceleration distance reaches $1[m]$.

It is important to note that the pendulum system was modeled as an inertial load in the following tests and as thus, the excitation of the pendulum by the controllers is not investigated.

The first trajectory tested was a stepped reference input. The controller used in this test was very slow acting as it is purely designed to reach the targeted velocity at a distance of $1[m]$.

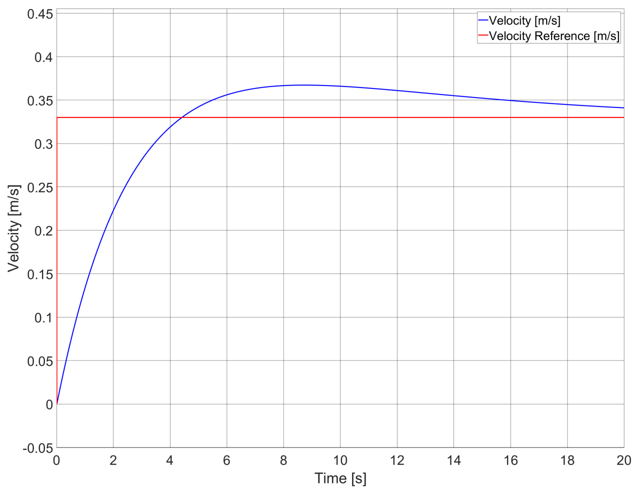

Fig. 7 Stepped reference velocity with low speed controllers prioritizing low currents.

The second trajectory tested was a constant acceleration of $[0.1m/s^2]$. This test uses a similar, low speed controller to the step input test.

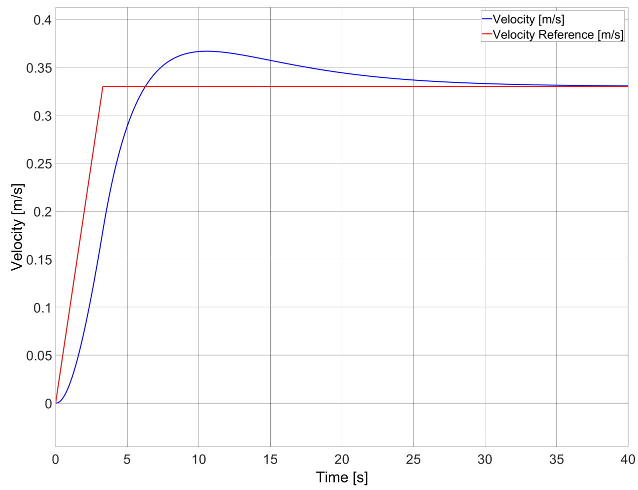

Fig. 8 Ramped reference velocity with low speed controllers prioritizing low currents.

In each of the tests, the power input to the motor is calculated and integrated to give the full energy required for the acceleration. In the stepped test, the energy required was $190[J]$, and in the ramped test, the system required $165[J]$. Both of these values neglect the power required to recover from the overshoot which leads to the necessity of a more ideal ramp.

In order to accelerate the system with as little wasted energy as possible, an ideal ramp is calculated using Equation 15.

$$\begin{aligned} \Delta x &= \frac{1}{2} \cdot a \cdot t^2 \\ \Delta x &= \frac{1}{2} \cdot a \cdot (\frac{v}{a})^2 \end{aligned} \tag{15}$$

When the ideal ramp is used, a significantly more aggressive controller can be used.

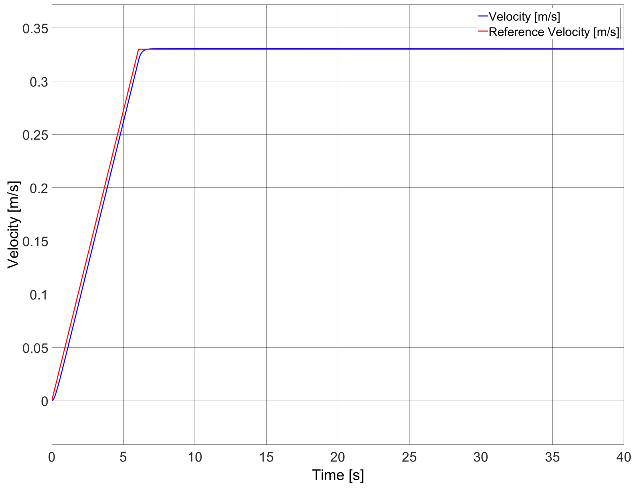

Fig. 9 Ideally ramped trajectory to operating speed with more aggressive controller.

As can be seen in Figure 9, the system reacts significantly more effectively with the combination of the ideal ramp and aggressive controller. The energy required to reach $0.33[m/s]$ in this test was calculated as $160[J]$ which while it is a minor improvement over the previous ramped tests, does not include the large amount of energy wasted on overshoot.

7.4 Disturbance Rejection

With the more aggressive controller from the ideal ramped test, the disturbance rejection of the system was tested with track slopes defined by a white noise input of amplitude $\pm 1.5°$ which approximately is a slope of $\pm 2\%$ grade.

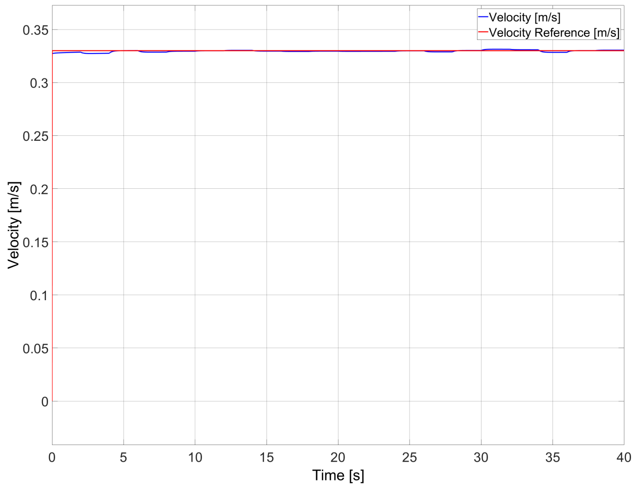

Fig. 10 Constant velocity reference with white noise disturbances.

The controller is seen to be very effective at rejecting the disturbances however the behavior with the pendulum is yet to be seen.

7.5 Testing on MagicPie Motor

The control of the motor was tested on the physical system through the use of the inverter board discussed in section 8. Through these tests, the motors top speed of $178[rpm]$ was confirmed as well as the capability of the controllers to maintain the torque necessary to accelerate under a load while minimizing the excess current.

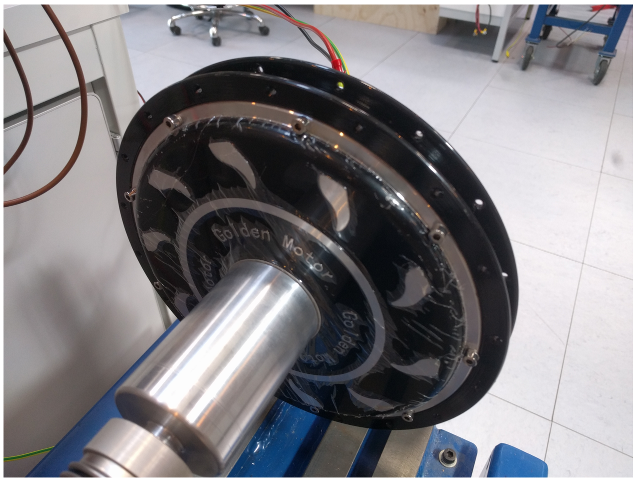

Fig. 11 The test setup with the MagicPie motor.

Note that the testing was conducted with a resistive load across another PMSM and not with the trolley system.

8. Implementation

In order to test the control of the hub motor, the control of the system was implemented in an embedded application through the use of the inverter board pictured in figure 12.

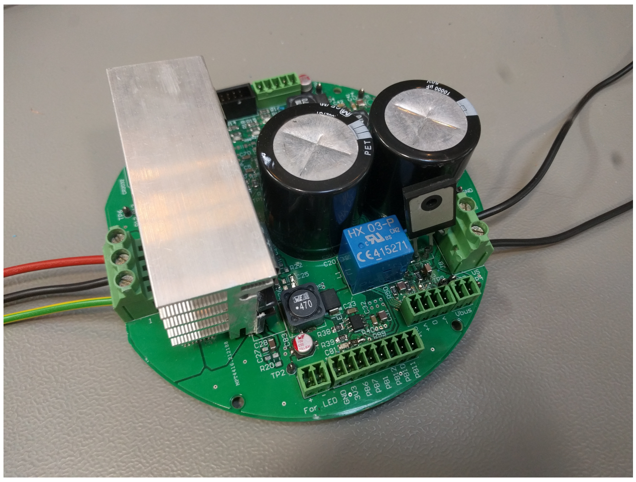

Fig. 12 Inverter Board.

The inverter board used in the testing of the motor consists of a motor gate driver, an STM32F103 micro-controller, analog current sensors, and dc supplies to drive them all. The full board is provided with $24[V]$ and a maximum of $6[A]$ DC as the current sensors have a limited measuring range of $6[A]$ per phase.

The STM32F103 microcontroller was programmed in C using the standard peripheral libraries.

8.1 Hall Effect Sensors

The MagicPie motor includes position feedback in the form of integrated hall effect sensors to give the location of the magnetic field in the motor. With the hall effect sensors giving 6 pulses per electrical period of the motor, the feedback has a resolution of 138 divisions per rotation.

In order to use the hall effect sensors, an additional circuit had to be attached as the on-board components did not produce a signal with an amplitude readable by the microcontroller. As the hall effect sensors used in the motor ground the signal when active, a pull-up resistor for each channel as well as a filtering capacitor were necessary to provide a clean signal. In addition, an external supply for the $3.3[V]$ power to the sensors was used as the power supplied by the board did not maintain a signal with the proper amplitude.

8.2 Position Measurement

In order to measure the position of the rotor, the hall effect sensor states are measured when they trigger an external interrupt. The interrupt is triggered on both the rise and fall of the signal in order to give a resolution of $\frac{2\pi}{6}$. As this resolution is too low to accurately generate sine waves from, the measured angular velocity in the last period of the hall effect signals is used to project the position for the next period.

This method utilizes TIM3 and TIM4 to measure the speed and to update the sine waves. When an interrupt is triggered, the hall effect sensors are measured and depending on the state, in the range 1-7, the position is updated. The value of t_{omega}, the time it takes the motor to travel between hall effect sensors, is then updated as the value of the TIM3 counter, and the counter is reset. The value of t_{omega} is thus inversely proportional to the angular velocity. The PWM duty cycle is updated based on this value by setting the TIM4 period to $\frac{1}{52}$ of the t_{omega} value. The period is set to this value as the sine wave look-up table has 314 values in each period and an update rate greater than that is unnecessary. On each interrupt of TIM4, the value of the output is calculated and the position iterated by one.

8.3 Sinewave Generation

The sine and cosine functions are handled through a look-up table with 314 values per period and are wrapped in conditional statements that increment or decrement the value if the angle is out of range of the table. The values in the look-up table are in the range of 0 to 255.

The PWM generation is handled by TIM1 which drives the PWM1 peripheral that, on the STM32F103 chip can produce three separate PWM signals as well as the inverse of the signals. The PWM timer is set as an up-down counter and has a period of 256 clock cycles. Upon each interrupt of TIM1, the period of each PWM signal is updated to the values of A, B, and C.

A dead time of 5 PWM clock cycles was used however the effects of modifying this value was not tested for the effects on efficiency.

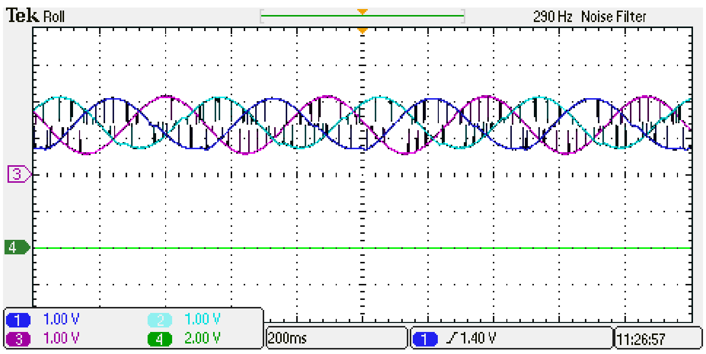

Fig. 13 Sine wave output from the microcontroller.

The duty cycle of the sine waves is updated at a synchronous rate with the velocity of the motor. As previously mentioned, the PWM is updated whenever the TIM4 interrupt is triggered. The TIM4 period is defined as $\frac{1}{52}$ of the time taken to travel to the current hall effect sensor from the last one. The value of $\frac{1}{52}$ is chosen as it is approximately one sixth of the 314 values in the sine look-up table. As the number of values is not directly divisible by six, there are some spikes in the sine wave output when the value jumps. As thus, increasing the number of values in the sine wave look-up table is a high priority for future code versions.

The discretization of the sine wave signal has not been observed to cause instability of the motor, however further testing must be conducted to identify the torque ripple.

9. Conclusion

The objective of this project was to implement and control a permanent magnet synchronous motor in the drive module of an automated feeding wagon. The result of the concept design was to replace the currently implemented DC motor and the gearbox with a high pole count hub motor with a rated torque high enough to make a gearbox unnecessary.

A nonlinear model of the current design was set up and tests were done to identify the energy losses so that the efficiency could be determined. Four tests were conducted, three no-load tests to determine the losses within the motor, gearbox, and belt drive, as well as one loaded test to determine the loaded frictional losses of the gearbox.

To compare the efficiency, a model of the system with the PMSM implemented was created. To validate the model of the PMSM performance tests were conducted to confirm the compliance of the model to the values stated in the datasheet and the values confirmed in testing of the actual motor. The peak velocity was found to be nearly identical between the datasheet, physical motor, and model as was the torque though the physical motor could not be tested with a high enough load or current to identify the peak torque.

To control the system cascade control was used. Separate PI controllers were used to control the direct and quadrature axis currents, and a slower PI controller for the velocity.

Various speed controllers were developed for the system by targeting the operation requirements of 0.33 $[m/s]$ and acceleration to the operating speed within a distance of 1 $[m]$. The initial controllers were designed to target these requirements by achieving the target velocity at the distance limit, thus minimized the energy needed. These controllers were tested with various step reference inputs and ramped reference inputs. In order to further improve the behavior of the system, an ideal reference ramp was calculated so that a more aggressive controller could be utilized to maintain a constant acceleration. With this controller, near constant acceleration, 0% overshoot, and effective disturbance rejection were observed.

As a result of the project an improved transmission system was designed, controllers for the permanent magnet synchronous motor were developed and the controllers implemented in embedded software to be tested on a physical system. The results in terms of control look promising, however further investigation is necessary in terms of the energy losses in the system.

Acknowledgement

The authors of this work gratefully acknowledge Grundfos for sponsoring the 6th MechMan symposium.

References

[1] P. C. SEN, Principles of Electric Machines and Power Electronics. No. ISBN: 0-471-02295-0 in 2nd edition, John Wiley & Sons Inc, 1998. page 121-153.

[2] R. K. P. PILLAY, Transactions on Industrial Electronics. No. electronic ISSN: 1557-9948 in vol 35 no. 4, IEEE, 1988. page 537-541.

[3] J. M. P. Charles L. Philips, Feedback Control Systems. No. ISBN-13: 978-0-13-186614-0 in 5nd edition, Pearson, 2011.

[4] T. L. SKVARENINA, Power Electronic Handbook Industrial Electronics Series. No. ISBN: 0-8493-7336-0, CRC Press, 2002. chapter 12-3.